Aftershock study and seismotectonic implications of the 8 March 2010 Kovancılar (Elazığ, Turkey) earthquake (M_W = 6.1)

Onur Tan,[1] Zümer Pabuçcu,[1] M. Cengiz Tapırdamaz,[1] Sedat İnan,[1] Semih Ergintav,[1] Haluk Eyidoğan,[2] Ercan Aksoy,[3] and Fatih Kuluöztürk[4,5]

Received 7 April 2011; revised 25 April 2011; accepted 25 April 2011; published 11 June 2011.

[1] A destructive earthquake (M_w = 6.1) occurred on the northeast end of the Palu segment of the East Anatolian Fault System (EAFS, eastern Turkey) on 8 March 2010. The spatial distribution of aftershocks suggests that the Palu segment does not terminate to the east of Palu town but extends in the N50°E direction where it has produced a 30 km right stepover. Aftershock depths indicate a seismogenic brittle zone of about 15 km depth. The stress changes on the segments due to recorded events might have loaded more than 0.5 bars of stress on the NE end of the Palu segment and the SW end of the Göynük segment. Therefore, a future earthquake on both segments may occur sooner than was expected before the occurrence of the M_w 6.1 earthquake on 8 March 2010. **Citation:** Tan, O., Z. Pabuçcu, M. C. Tapırdamaz, S. İnan, S. Ergintav, H. Eyidoğan, E. Aksoy, and F. Kuluöztürk (2011), Aftershock study and seismotectonic implications of the 8 March 2010 Kovancılar (Elazığ, Turkey) earthquake (M_W = 6.1), *Geophys. Res. Lett.*, *38*, L11304, doi:10.1029/2011GL047702.

1. Introduction

[2] The Kovancılar earthquake (M_W = 6.1) occurred on 8 March 2010 (02:32 UTC) in Elazığ province, eastern Turkey (Figure 1a). The earthquake was strongly felt in both Elazığ and Bingöl provinces. Approximately one hundred villages were affected; more than 4,000 buildings were heavily damaged and the number of fatalities was reported to be 42. One day after the mainshock, we established six temporary seismic stations around the epicenter to collect aftershock data (aftershock studies were funded by the Turkish State Planning Organization (SPO) -supported "Urgent Monitoring Studies Project" [see *Tan et al.*, 2010]). Recording of aftershock activity started on 10 March and continued until 30 May 2010.

[3] The Kovancılar earthquake occurred between the Palu and Göynük segments of the East Anatolian Fault System (EAFS) that extends from Kahramanmaraş in the southwest to Karlıova in the northeast [*Arpat and Şaroğlu*, 1972]. The EAFS is a left-lateral strike-slip fault system, and together with the widely known the North Anatolian Fault System (NAFS), facilitates the western escape of the Anatolian Plate [*Şengör and Yılmaz*, 1981]. There are also several segments oblique to the main fault [*Bozkurt*, 2001] (Figure 1a). The pull-apart basins and stepovers in the region are the geological evidence of a complex fault zone. The Palu and Göynük segments of the EAFS are traced clearly in the field [*Arpat and Şaroğlu*, 1972; *Şaroğlu et al.*, 1992; *Herece*, 2008] (Figure 1a). *Arpat and Şaroğlu* [1972] moreover mapped several folding structures related to the Gökdere Uplift (GU) formed by a right stepover of the Palu segment [*Arpat and Şaroğlu*, 1972; *Herece*, 2008]. The Palu segment follows the boundary between the Elazığ magmatics and Lutetian-Chattian conglomerates and aftershocks locate mostly on this boundary (Figure 1b).

[4] Several large historical earthquakes (M > 7) occurred on the EAFS, in addition a few moderate events (i.e., 1986 Sürgü and 1971, 2003 Bingöl) have occurred in the instrumental period. On the other hand, no seismological study has been undertaken for the area between the town of Palu and the Bingöl city center. Thus, the Kovancılar earthquake and its aftershocks provided new opportunities to study in this area.

2. Data and Methods

[5] Six temporary seismic stations were deployed in the earthquake area to monitor the aftershock activities (Figure 1b). Each station was equipped with three components geophone, Reftek-130 recorder and a GPRS modem. All stations acquired continuous data at 100 samples per second (sps) between 10 March and 30 May 2010. Additionally, we used on-line broadband stations of the TURDEP project [*İnan et al.*, 2007] to analyze the events ($M_L \geq 3.0$). The parameters of the events that occurred before the deployment of the local network were determined using the broadband stations of the TURDEP project and the national networks. The absolute hypocentral parameters of the earthquakes were computed with the *Hypocenter* location algorithm described by *Lienert and Havskov* [1995]. The average horizontal and vertical uncertainties of the ~2130 aftershocks ($M_L \geq 0.3$) were found to be 3 and 4 km, respectively. We worked to reduce these uncertainties.

[6] In minimizing the errors in the location parameters, network geometry, phase reading quality and uncertainties in the crustal structure are limiting factors. Relative earthquake location methods can improve absolute hypocenter locations. For this purpose, we used the double-difference algorithm (*hypoDD*) developed by *Waldhauser and Ellsworth* [2000]. The algorithm assumes that the difference in travel times for two close events observed at one station can be attributed to the spatial offset between the events with high accuracy. We

[1]Earth and Marine Sciences Institute, TÜBİTAK Marmara Research Center, Gebze, Turkey.
[2]Department of Geophysical Engineering, İstanbul Technical University, Istanbul, Turkey.
[3]Department of Geological Engineering, Elazığ Fırat University, Elazığ, Turkey.
[4]Department of Physics, Elazığ Fırat University, Elazığ, Turkey.
[5]Department of Physics, Bitlis Eren University, Bitlis, Turkey.

Published in 2011 by the American Geophysical Union.

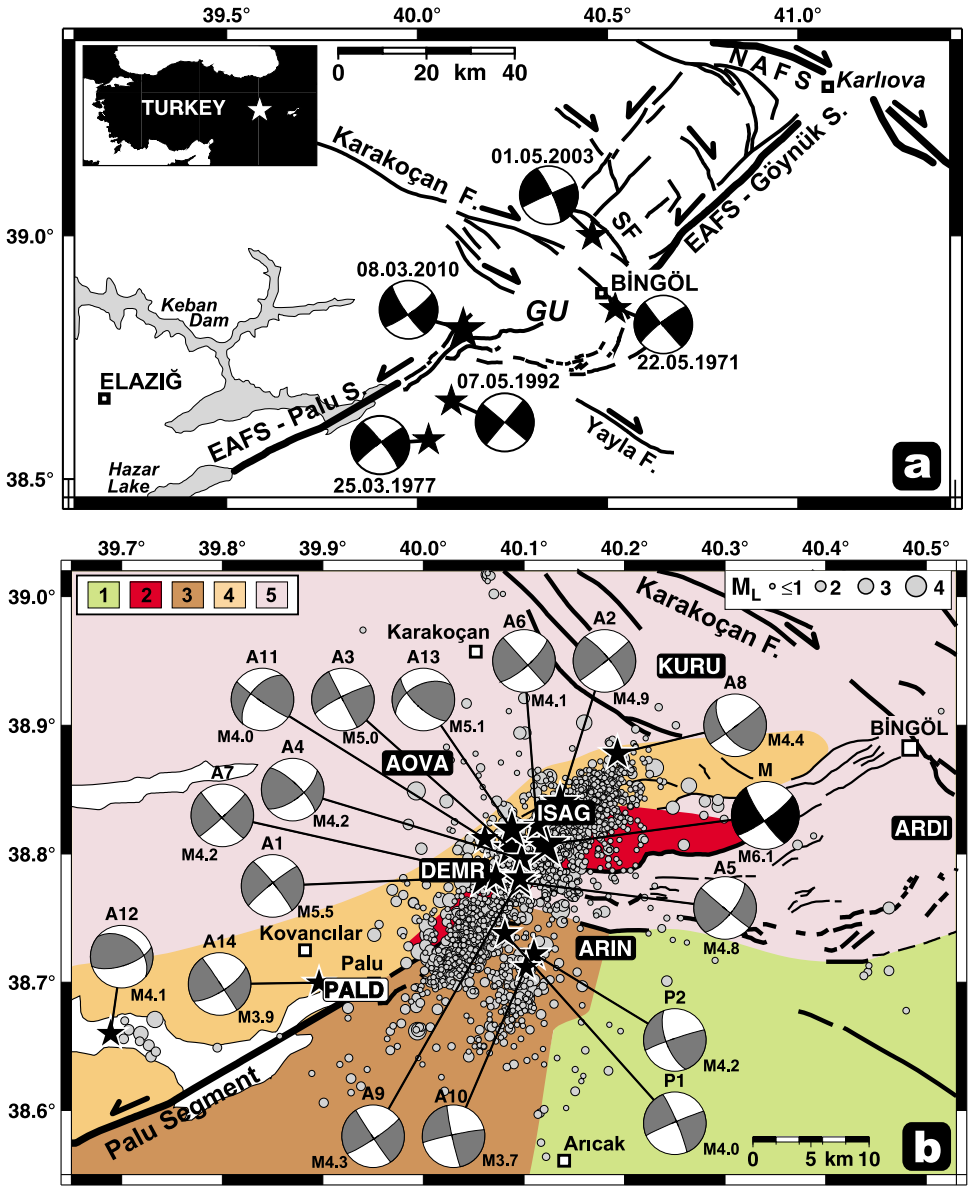

Figure 1. (a) The faults and earthquakes (M > 5.5) in the study area [*Şaroğlu et al.*, 1992; *Emre et al.*, 2010; *Tan et al.*, 2008]. EAFS: East Anatolian Fault System, GU: Gökdere Uplift, NAFS: North Anatolian Fault System, SF: Sudüğünü Fault. (b) The aftershock activity of the Kovancılar earthquake (*M*) and the focal mechanisms of the large preceding events (*P*) and aftershocks (*A*). The moment magnitudes (M_W) are given beneath the focal spheres. Stations are shown with black labels (i.e., KURU). The geological units are also shown: 1: Pütürge metamorphics (Precambrian), 2: Elazığ magmatics (Upper Cretaceous), 3: Conglomerate/Sandstone (Maastrichtian), 4: Conglomerate (Lutetian-Chattian), 5: Andezit/Bazalt (Pliocene) (simplified from *Herece*, 2008).

used absolute location parameters of the events and the *P/S* travel time differences between the event pairs as the inversion inputs. Additionally, *P/S*-wave cross-correlation data were also used. The waveform similarities of the events were determined with the coherence algorithm of the *MTSPEC* package of *Prieto et al.* [2009]. Two waveforms recorded at a common station were considered similar when 70% of the squared coherency values exceed 0.7. We improved the location of approximately half of the aftershocks. The location uncertainties after the final double-difference inversion were estimated using the statistical approach described by *Tan et al.* [2010]. Accordingly, randomly shifted event pairs were re-located with the 1000 well-conditioned inversions. The location scatterings according to the final locations suggest that horizontal and vertical location errors are less than ±750 m and ±1000 m, respectively.

[7] The fault mechanism solutions of the events ($M_L \geq 3.5$) were determined with both *P*-wave polarities and the local moment tensor inversion algorithm. Only the seismograms that were recorded by stations located between 30 and 200 km were used for the solutions implemented with the *ISOLA* local moment tensor inversion algorithm [*Sokos and Zahradnik*, 2008]. At least four stations and three components waveforms filtered between the frequency bands of

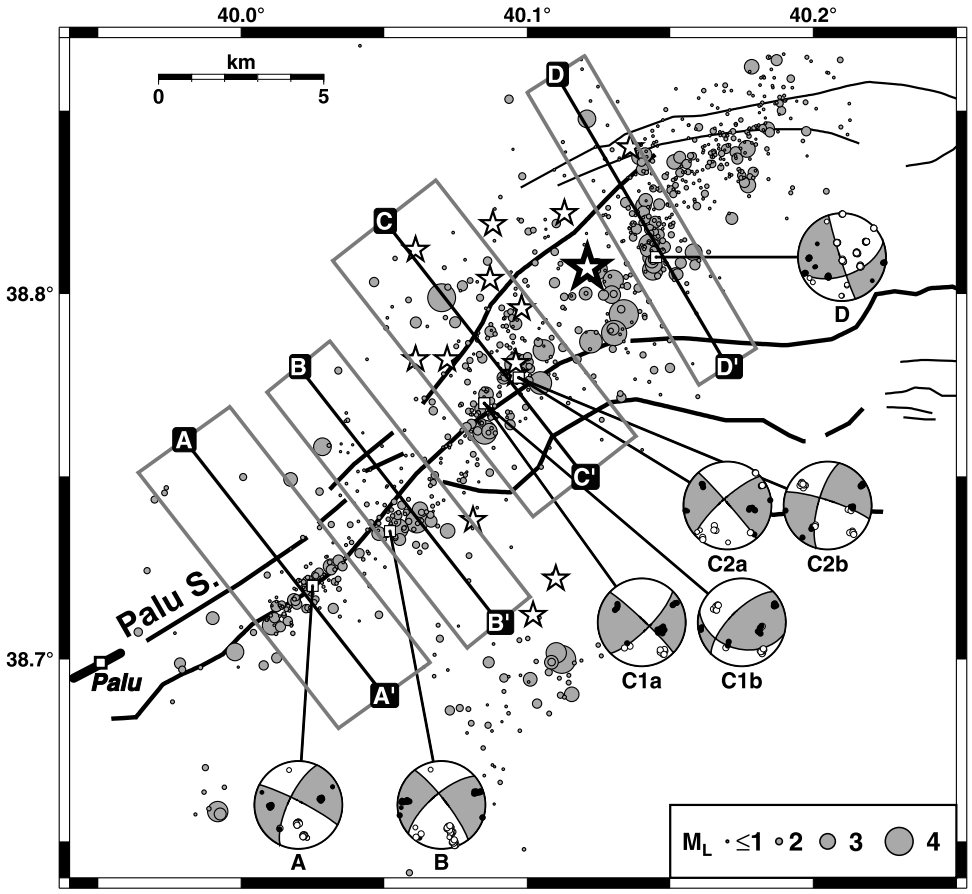

Figure 2. The high-resolution micro-earthquake locations after the *hypoDD* analysis. A, B, C and D are the cross-section profiles, and grey rectangles indicate event selection areas. The JFMS with polarities of the clusters are also shown. Stars are the mainshock and large aftershocks in Figure 1b. The thick and thin lines are faults and folds axis, respectively [*Emre et al.*, 2010].

0.03 Hz – 0.1 Hz were inverted for events. On the other hand, the joint focal mechanism solutions (JFMS) of selected micro-earthquakes in a small volume were determined using the *focmec* program [*Snoke et al.*, 1984]. Finally, based on the reliable data, we also calculated the rupture area [*Kanamori*, 1977; *Mai and Beroza*, 2000] and conducted failure analysis using the computer algorithm *Coulomb 3.0* [*Lin and Stein*, 2004; *Toda et al.*, 2005]; keeping in mind that the computed failure stress changes of less than one bar is generally sufficient to explain the aftershock distributions [*King et al.*, 1994].

3. The Earthquake Sequence

[8] The location (38.807°N 40.121°E ± 5 km, h = 5 ± 4 km) and the fault plane solution (strike 54°, dip 80°, rake −10°) of the mainshock indicate that the rupture process developed on an almost pure left-lateral strike-slip fault; the rupture originated at the location about 20 km NE of Palu (Figure 1b). 22 days before the mainshock, two events (*P1*, *P2*; $M_W \geq 4$) with strike-slip mechanisms were recorded to the south of the mainshock area. Near the vicinity of the mainshock, 12 major aftershocks (*A1* to *A12* shown in Figure 1b), $M_W \geq 4$, were recorded during the observation period. The mechanism solutions of these aftershocks are in good agreement with that of the mainshock; all indicating left-lateral strike-slip faulting in NE-SW orientation. The faulting parameters of these events are given in the auxiliary material.[1]

[9] The aftershock activity in the observation period between 10 March and 30 May 2010 extends from the east of the town of Palu to the southwest of the station KURU; in approximately 25 km NE-SW direction (Figure 1b). The depths of the aftershocks varied between 5 and 20 kilometers.

[10] Another distinctive cluster was observed in the area of two major aftershocks (*P2* and *A10*); both aftershocks show that this cluster occurred on a strike-slip fault segment. The moment tensor inversion of one aftershock (*A12*) located in the Keban Dam Lake indicates a reverse faulting mechanism. One of the largest aftershocks (*A13*, M_L = 5.1) also indicates reverse faulting mechanism with minor strike-slip component.

[11] As the output of the *hypoDD* analysis, 995 aftershocks (out of ~2130 aftershocks) were determined to be highly accurate. The location and faulting process become more apparent after the double-difference inversion of the aftershock data (Figure 2). Improved aftershock locations

[1] Auxiliary materials are available in the HTML. doi:10.1029/2011GL047702.

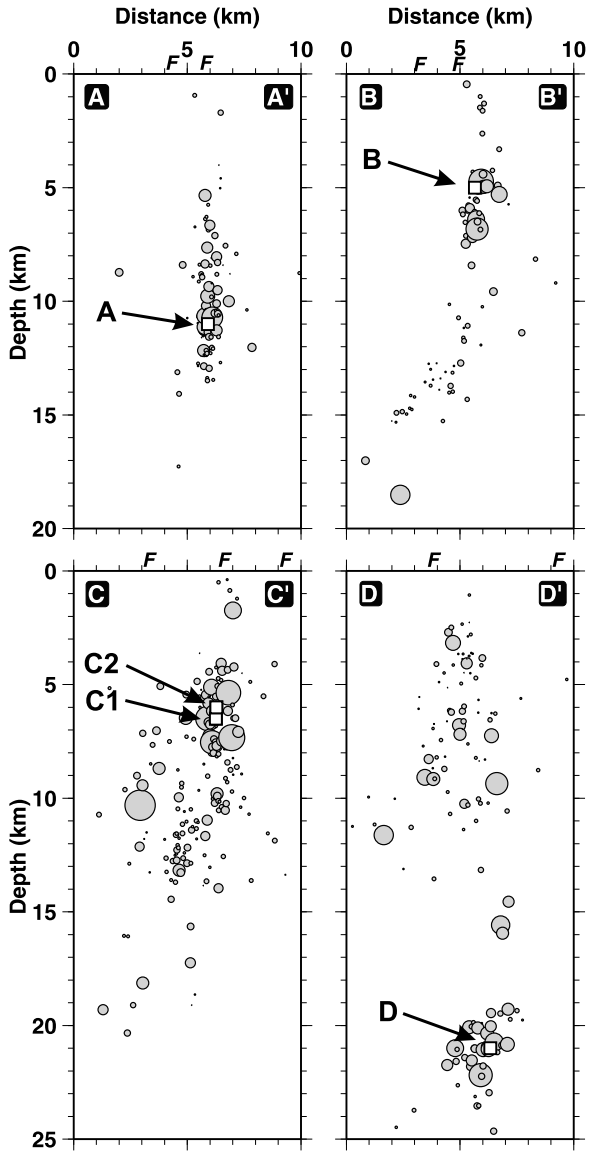

Figure 3. Cross-sections for the profiles given in Figure 2. *F* denotes fault segment observed in the field [*Emre et al.*, 2010].

and depths yielded a better picture of seismicity; shedding light about the thickness of the seismogenic (brittle) crust. Moreover, fault plane solutions as will be shown next helped in identifying the fault slip motion.

[12] In the southernmost end of the activity (cluster A), the seismicity occurred in a very narrow zone (~1 km) and the depths of the earthquakes were found to be between 5 and 12 km (Figure 3). The JFMS of selected 15 events ($2.8 \geq M_L \geq 1.1$, 61 *P*-wave polarities) in a sphere with radius (*r*) of 1 km indicate a fault segment with left-lateral strike-slip character in the cluster A. Cluster B covers the aftershocks occurring at depths of 5 and 7 km. The JFMS of 17 events ($3.4 \geq M_L \geq 1.1$, 69 pol., $r = 1.5$ km) verifies pure strike-slip faulting in this area. The dip angle of the NE-SW nodal plane is in good agreement with the slope of the focal depths on the B-B′ cross-section in Figure 3. These data show that the fault dip is 70°–80°NW. The mainshock and the large aftershocks occurring in the first two days after the mainshock also occurred in this area (profile C and D in Figure 2). It is worth noting that several micro-earthquakes show two different mechanisms in a relatively small volume ($r = \sim 1$ km). For example, the events in the cluster C1 ($1.9 \geq M_L \geq 1.1$, 28 pol.) group into left-lateral strike slip (C1a) and reverse (C1b) mechanisms at the same point on the fault surface. The cluster C2 ($3.7 \geq M_L \geq 1.7$, 35 pol.) also shows well-constrained strike-slip faulting solutions. The 104 *P*-wave polarities from the deepest cluster D ($3.4 \geq M_L \geq 1.8$, 8 events) are also in good agreement and indicate a strike-slip mechanism.

4. Discussions and Conclusions

[13] There are three known historical large earthquake on the Palu and Göynük segments. The locations of the historical 1789, 1874 (M = 7.1) and 1875 (M = 6.7) earthquakes are reported to have occurred on this segment [*Ambraseys and Jackson*, 1998]. The other important historical event (Ms = 7.2) occurred in 1866 on the Göynük Segment with more than 45 km surface rupture [*Ambraseys*, 1997]. In the instrumental period, no major earthquake activity has occurred on the Palu segment (Figure 1a). However, the 1971 Bingöl Earthquake ($M_w = 6.4$, Figure 1a) occurred on the Göynük segment [*Arpat and Şaroğlu*, 1972; *Jackson and McKenzie*, 1984; *Taymaz et al.*, 1991]. The surface rupture of this earthquake terminated at about 8 km NE of Bingöl. The field evidence and seismological data suggest that the 1971 Bingöl earthquake occurred on a left-lateral strike-slip fault. *Nalbant et al.* [2002] proposed that the area between Elazığ and Bingöl cities may generate destructive earthquake because of the stress change after the large earthquakes. Then, 1 May 2003 Bingöl earthquake ($M_W = 6.3$) occurred on the right lateral Sudüğünü Fault (SF) that is conjugate to the EAFS [*Milkereit et al.*, 2004; *Tan et al.*, 2008]. Although *Milkereit et al.* [2004] suggested that this event occurred because of the previous large historical earthquakes, *Nalbant et al.* [2005] concluded that the stress accumulation on the 2003 rupture area may be due to complex tectonic loading.

[14] The fault mechanism solutions of the Kovancılar earthquake and the high-resolution aftershock locations suggest that only the southwestern half of the aftershock dominated area has displayed pure left-lateral strike-slip motion (Figure 2). The central part of the activity shows not only strike-slip mechanisms but also there are aftershocks with thrust faulting solutions. These thrust mechanisms may occur due to the local stress change in the area after the mainshock. The seismological data in this study show that the Kovancılar earthquake occurred on a fault segment that may be the continuation of the Palu segment. On the other hand, the aftershocks in the northeastern part of the activity indicate that several small fault segments exist in this area. These small faults may have different faulting mechanisms (i.e., event *A13*).

[15] Our aftershock study following 1 May 2003 Bingöl earthquake ($M_W = 6.3$) indicated that all the aftershocks were shallower than 15 kilometers (TÜBİTAK MRC, unpublished report, 2003). However, similar findings were reported by *Milkereit et al.* [2004]. Therefore, we speculate that the thickness of brittle seismogenic crust in Bingöl area

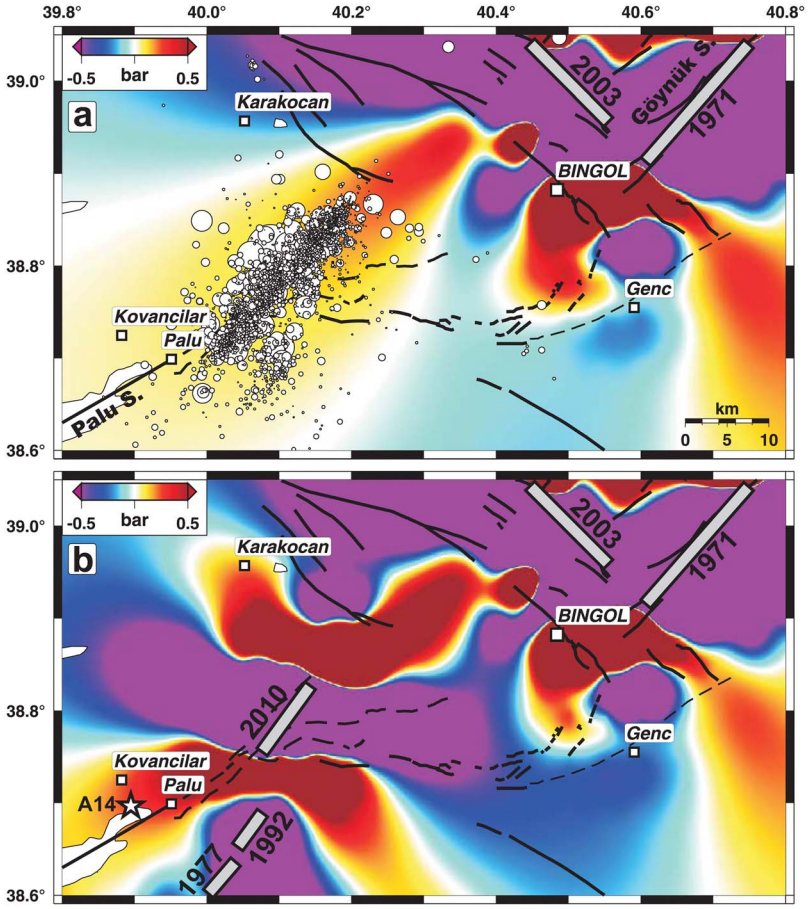

Figure 4. Coulomb stress changes on the specified left-lateral faults (strike 55°, dip 85°, rake 1°). (a) The stress load after the 1971 and 2003 Bingöl earthquakes. The circles are the epicenters of the 8 March 2010 Kovancılar earthquake sequence. (b) Cumulative stress changes after the five moderate events (M > 5, Figure 1a). The ruptured segments are shown with scaled rectangles. The star is the event *A14* (M_L = 4.0).

is about 15 kilometers. Our recent aftershock study of the Kovancılar earthquake also show that majority of the aftershocks occurred in the crust shallower than 15 km with the exception of few indicating about 20–25 km (cluster D). In parallel to latter findings, *Turkelli et al.* [2003] also noted that some earthquakes along the EAFZ, the Bitlis Suture Zone, the Karlıova junction area and the area east of Karlıova yielded hypocenters in the lower crust (h > 20 km).

[16] The geological and seismological observations show that the direction of the Palu and Göynük segments are about N60°E and N50°E, respectively. The recent activity is taken to imply that the Palu segment of the EAFS changes its direction to N50°E and becomes parallel to the Göynük segment. A 30 km stepover of the left-lateral segments, mentioned in previous studies, may lead to compression in the area between Palu and Bingöl. We have shown that the region to the west of the Gökdere uplift is seismically active and is capable of generating destructive earthquakes. However, we could not observe significant micro-earthquake activity in the Gökdere uplift during the observation period.

[17] The seismic moment of the 8 March 2010 mainshock ($M_o = 1.2 \times 10^{18}$ Nm) implies that the probable rupture area is 10×8 km^2. The calculated average displacement is 0.5 meters and stress-drop is about 40 bars [*Kanamori*, 1977; *Mai and Beroza*, 2000]. The spatial coverage of the aftershocks in the NE-SW direction is about 25 km. The Coulomb stress changes after the 1971 and 2003 Bingöl earthquakes show stress rise in the area of the Kovancılar earthquake (Figure 4a). The stress changes calculation on this segment of the EAFS using all instrumentally recorded destructive events in the region cause more than 0.5 bars of stress loads on the NE end of the Palu segment and the SW end of the Göynük segment in Bingöl (Figure 4b). This calculation agrees with the event *A14* (M_L = 4.0) that took place in the center of Palu town eight months after the Kovancılar earthquake. The stress load caused by the Kovancılar earthquake may have shortened the time for future earthquakes on either one of these segments.

[18] **Acknowledgments.** This project (DEPAR) was supported by the State Planning Organization of Turkey (SPO) and TÜBİTAK Marmara Research Center. This study has been also supported by the TURDEP project (TÜBİTAK 105G019). We thank Boğaziçi University Kandilli Observatory and Earthquake Research Institute for additional waveform data. We appreciate the interest and support of Mahmut Doğru, the Rector of Bitlis Eren University. We appreciate the help by the GRL editorial office for handling and language corrections. We also thank the GRL Editor, Ruth Harris, the reviewer A. Hubert-Ferrari and one anonymous reviewer for careful reviews and constructive comments on the manuscript. The earthquake waveform

data are stored on TÜBİTAK ULAKBİM TR-Grid system. The maps were drawn with the Generic Mapping Tools [*Wessel and Smith*, 1998].

References

Ambraseys, N. N. (1997), Little-known earthquakes of 1866 and 1916 in Anatolia (Turkey), *J. Seismol.*, *1*, 289–299, doi:10.1023/A:1009788609074.

Ambraseys, N. N., and J. Jackson (1998), Faulting associated with historical and recent earthquakes in the eastern Mediterranean, *Geophys. J. Int.*, *133*, 390–406, doi:10.1046/j.1365-246X.1998.00508.x.

Arpat, E., and F. Şaroğlu (1972), Some observations and thoughts on the East Anatolian fault [in Turkish], *Bull. Miner. Res. Explor. Inst. Turkey*, *73*, 44–50.

Bozkurt, E. (2001), Neotectonics of Turkey—A synthesis, *Geodin. Acta*, *14*, 3–30, doi:10.1016/S0985-3111(01)01066-X.

Emre, Ö., T. Y. Duman, S. Özalp, and H. Elmacı (2010), 8 March 2010 Başyurt-Karakoçan (Elazığ) earthquake [in Turkish], report, Miner. Res. and Explor. Inst. Turkey, Ankara.

Herece, E. (2008), *Atlas of East Anatolian Fault (EAF)*, *Spec. Publ. Ser.*, vol. 13, Miner. Res. and Explor. Inst. of Turkey, Ankara.

İnan, S., S. Ergintav, R. Saatçılar, B. Tüzel, and Y. İravul (2007), Turkey makes major investment in earthquake research, *Eos Trans. AGU*, *88*(34), doi:10.1029/2007EO340002.

Jackson, J., and D. McKenzie (1984), Active tectonics of the Alpine-Himalayan Belt between western Turkey and Pakistan, *Geophys. J. R. Astron. Soc.*, *77*, 185–264.

Kanamori, H. (1977), The energy release of great earthquakes, *J. Geophys. Res.*, *82*, 2981–2987, doi:10.1029/JB082i020p02981.

King, G. C. P., R. S. Stein, and J. Lin (1994), Static stress changes and the triggering of earthquakes, *Bull. Seismol. Soc. Am.*, *84*, 935–953.

Lienert, B. R. E., and J. Havskov (1995), A computer program for locating earthquakes both locally and globally, *Seismol. Res. Lett.*, *66*, 26–36.

Lin, J., and R. S. Stein (2004), Stress triggering in thrust and subduction earthquakes, and stress interaction between the southern San Andreas and nearby thrust and strike-slip faults, *J. Geophys. Res.*, *109*, B02303, doi:10.1029/2003JB002607.

Mai, P. M., and G. C. Beroza (2000), Source scaling properties from finite-fault-rupture models, *Bull. Seismol. Soc. Am.*, *90*, 604–615, doi:10.1785/0119990126.

Milkereit, C., H. Grosser, R. Wang, H.-U. Wetzel, H. Woith, S. Karakisa, S. Zunbul, and J. Zschau (2004), Implications of the 2003 Bingol earthquake for the interaction between the North and East Anatolian faults, *Bull. Seismol. Soc. Am.*, *94*, 2400–2406, doi:10.1785/0120030194.

Nalbant, S. S., J. McCloskey, S. Steacy, and A. A. Barka (2002), Stress accumulation and increased seismic risk in eastern Turkey, *Earth Planet. Sci. Lett.*, *195*, 291–298, doi:10.1016/S0012-821X(01)00592-1.

Nalbant, S. S., J. McCloskey, and S. Steacy (2005), Lessons on the calculation of static stress loading from the 2003 Bingol, Turkey earthquake, *Earth Planet. Sci. Lett.*, *235*, 632–640, doi:10.1016/j.epsl.2005.04.036.

Prieto, G. A., R. L. Parker, and F. L. Vernon III (2009), A Fortran 90 library for multitaper spectrum analysis, *Comput. Geosci.*, *35*, 1701–1710, doi:10.1016/j.cageo.2008.06.007.

Şaroğlu, F., Ö. Emre, and İ. Kuşçu (1992), *Active fault map of Turkey [in Turkish]*, Miner. Res. and Explor. Inst. of Turkey, Ankara.

Şengör, A. M. C., and Y. Yılmaz (1981), Tethyan evolution of Turkey: A plate tectonic approach, *Tectonophysics*, *75*, 181–241, doi:10.1016/0040-1951(81)90275-4.

Snoke, J. A., J. W. Munsey, A. G. Teague, and G. A. Bollinger (1984), A program for focal mechanism determination by combined use of polarity and SV/P amplitude ratio data, *Earthquake Notes*, *55*(3), 15.

Sokos, E., and J. Zahradnik (2008), ISOLA a Fortran code and a Matlab GUI to perform multiple-point source inversion of seismic data, *Comput. Geosci.*, *34*, 967–977, doi:10.1016/j.cageo.2007.07.005.

Tan, O., M. C. Tapırdamaz, and A. Yörük (2008), The earthquake catalogues for Turkey, *Turk. J. Earth Sci.*, *17*(2), 405–418.

Tan, O., et al. (2010), Bala (Ankara) earthquakes: Implications for shallow crustal deformation in central Anatolian section of the Anatolian platelet (Turkey), *Turk. J. Earth Sci.*, *19*, 449–471, doi:10.3906/yer-0907-1.

Taymaz, T., H. Eyidogan, and J. A. Jackson (1991), Source Parameters of large earthquakes in the East Anatolian Fault Zone (Turkey), *Geophys. J. Int.*, *106*, 537–550, doi:10.1111/j.1365-246X.1991.tb06328.x.

Toda, S., R. S. Stein, K. Richards-Dinger, and S. B. Bozkurt (2005), Forecasting the evolution of seismicity in Southern California: Animations built on earthquake stress transfer, *J. Geophys. Res.*, *110*, B05S16, doi:10.1029/2004JB003415.

Turkelli, N., et al. (2003), Seismogenic zones in eastern Turkey, *Geophys. Res. Lett.*, *30*(24), 8039, doi:10.1029/2003GL018023.

Waldhauser, F., and W. L. Ellsworth (2000), A double-difference earthquake location algorithm: Method and application to the northern Hayward fault, California, *Bull. Seismol. Soc. Am.*, *90*, 1353–1368, doi:10.1785/0120000006.

Wessel, P., and W. H. F. Smith (1998), New, improved version of the Generic Mapping Tools released, *Eos Trans. AGU*, *79*, 579, doi:10.1029/98EO00426.

E. Aksoy, Department of Geophysical Engineering, Elazığ Fırat University, Elazığ 23119, Turkey.

S. Ergintav, S. İnan, Z. Pabuçcu, O. Tan, and M. C. Tapırdamaz, Earth and Marine Sciences Institute, TÜBİTAK Marmara Research Center, Gebze, Kocaeli 41470, Turkey. (onur.tan@mam.gov.tr)

H. Eyidoğan, Department of Geophysical Engineering, İstanbul Technical University, İstanbul 34469, Turkey.

F. Kuluöztürk, Department of Physics, Elazığ Fırat University, Elazığ 23169, Turkey.